Vol 3 No 1 (2021) *e*-ISSN: 2682-8383

Journal of Engineering Technology and Applied Physics

Effects of Anode Design and Configuration on the Growth Dynamics and Surface Morphologies of Electrodeposited Copper Films

Choo Kan Yeep[1,]*, Lim E Lin[1], Ong Duu Sheng[1] and You Ah Heng[2].
[1]*Faculty of Engineering, Multimedia University, Persiaran Multimedia, 63100, Cyberjaya, Selangor D.E., Malaysia.*
[2]*Faculty of Engineering and Technology, Multimedia University, Jalan Ayer Keroh Lama, 75450 Melaka, Malaysia.*
**Corresponding author*: kychoo@mmu.edu.my
https://doi.org/10.33093/jetap.2021.3.1.5
Manuscript Received: 22 Dec 2020, Accepted: 7 Jan 2021, Published: 15 June 2021

***Abstract* - The influence of different anode configurations on the growth mechanisms, transient currents and surface morphologies of copper film using localized electrodeposition technique have been studied. Measured transient currents during electrodeposition were used to investigate the underlying growth dynamics. SEM images were obtained and the surface morphologies of the deposited copper films were analyzed. It was found that the transient current increased when copper ions were able to grow directly on the empty surface of the copper film that was located away from the mini electrodes. This caused the copper ions to be deposited sporadically via the instantaneous growth mechanism and formed cluster of atoms on the empty surface of the copper film which led to rougher surfaces. In contrast, progressive growth was observed to occur at a faster rate for the deposition performed using insulated mini electrodes, especially in the case of collinear double insulated mini electrodes as indicated by the reduction of the transient current with time. Besides, copper films with uniform and smoother surfaces were obtained when the depositions were performed using multiple or a large number of closely spaced mini electrodes. This was due to the fact that large number of closely spaced mini electrodes produced parallel and uniform electric field patterns.**

Keywords* — *Copper film, miniature electrode, localized electrodeposition, instantaneous growth, progressive growth.

I. INTRODUCTION

Electrodeposition is a wet electrochemical process that uses either an electrical potential or current to cause ions of desired material to be deposited on a conducting substrate that is submerged in an electrolyte. When an ion arrives at the surface of the substrate, it diffuses on the surface before it establishes a bonding with the host atom on the substrate by receiving electrons that are populating on the surface of the substrate. Since the electrodeposition process involves the deposition of ions at the atomic level, this technique has many advantages and offers greater flexibility of realizing material film growth with thickness varying from a few atomic layers to a few millimeters.

Owing to the facts that electrodeposition is a versatile, low temperature, inexpensive and simple technique; it has become a promising growth technique for copper interconnect in the semiconductor interconnect technology and microelectronic industry [1-6]. In addition, superior abilities of this technique (i) to overcome the shadowing effect due to the high aspect ratio of the trenches or via that are present on the surface of the wafers and (ii) via-filling ability for the ultra-large scale integration interconnect have further strengthen

This work is licensed under the Creative Commons BY-NC-ND 4.0 International License.
Published by MMU PRESS. URL: https://journals.mmupress.com/index.php/jetap/index

the applicability of this technique in the semiconductor interconnect technology as compared to that of the commonly used techniques such as the chemical vapor deposition (CVD), sputtering and evaporation techniques.

In recent years, electrodeposition technique has been extensively developed for the realization of microstructures [7-9] and nanostructures [10-11] using patterned electrodes, pulse conditions or magnetohydrodynamic effects [12-17]. These techniques allow the growth and fabrication of planar or three-dimensional micrometer-scale and nanometer-scale structures without the necessity for lithography process. This could lead to reduction of production cost of electrodeposited structures. Moreover, localized deposition is also an additional feature viable for electrodeposition technique in which the deposition is restricted to a confined region. This could be achieved by placing a miniature electrode on top of a conductive substrate where both of them are immersed in an electrolyte solution. An electrical potential is then applied between the miniature electrode and the conducting substrate so that an electric field is established and constrained within the region between the electrode and substrate. Thus, the deposition takes place at the region beneath the tip of the electrode.

The objectives of this work are to investigate the influences of different designs and configurations of miniature electrodes on localized electrodeposition of copper. The measured transient currents during the deposition together with the scanning electron microscopy (SEM) images of the copper films are used to explain the underlying growth dynamics of the localized electrodeposition of copper.

II. EXPERIMENT SETUP AND MEASUREMENTS

Cathodes (or substrates) were made of square copper films with an area size of 5 mm × 5 mm. Each of these cathodes was connected with a 1 mm width tiny copper strip so that the substrate can be electrically connected to the circuit of the electrochemical cell as shown in the Fig. 1(a)(i). Anode (henceforth it is called as mini electrode) was made of a copper wire with diameter of 0.2 mm as shown in the Fig. 1(a)(ii). Two variants of the mini electrodes, namely the insulated and uninsulated mini electrodes were prepared for the experiments. The insulator of a cooper wire was entirely striped off to realize the uninsulated mini electrode so that the copper wire submerged in the electrolytes would be involved in the electrodeposition process. In contrast, insulated mini electrode was realized by stripping off a 2 mm length insulator from the end of a cooper wire so that the small expose copper wire could act as a sharp tiny tip in the electrodeposition process. Top views of the various designs and configurations of the copper mini electrodes used in the experiment are (i) single mini electrode, (ii) collinear double mini electrode with inter-electrode spacing of 2 mm and (iii) square quadruple mini electrode with inter-electrode spacing of 2 mm, in which the four mini electrodes are placed at the corner points of a square with width of 2 mm are shown in the Fig. 1(b). The oxide layers on the copper mini electrodes and substrates were removed by immersing them in the bath of sulfuric acid for 20 minutes. After that, they were rinsed with deionized water and blown dry with nitrogen gas. The electrolyte was prepared by dissolving copper sulfate pentahydrate ($CuSO_4 \cdot 5H_2O$) in warm deionized water to achieve a concentration of 100 g/l.

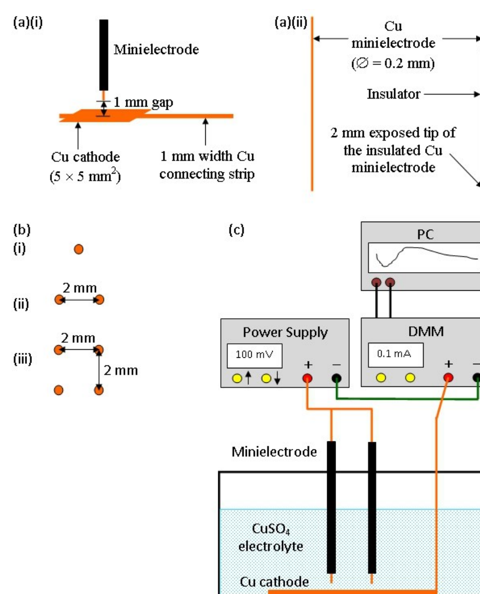

Fig. 1. (a)(i) Design of Cu substrate and (ii) Designs of insulated and uninsulated Cu mini electrodes; (b) Top views of the configurations of Cu mini electrodes: (i) single mini electrode, (ii) collinear double mini electrode (2 mm inter-electrode spacing), (iii) square quadruple mini electrode (2 mm inter-electrode spacing); (c) Experimental setup for the electrodeposition system.

All electrodeposition processes were carried out using a two-electrode electrochemical cell system as depicted in the Fig. 1(c). The cathode was connected to the negative terminal of the power supply and served as the substrate to receive the copper ions. Meanwhile, the mini electrode connected to the positive terminal of the power supply served as the source to replenish the copper ions. The substrate was placed horizontally on the bottom of the electrochemical cell and the mini electrode was positioned directly about 1 mm above the substrate. A Keithley 2000 digital multimeter (DMM) was connected in series with the mini electrode, substrate and power supply and configured in DC current measurement mode with shortest integration time so that the transient current resulted from the electrochemical cell could be recorded as fast as possible by a desktop computer to monitor the evolution of the deposition.

The deposition was first carried out with uninsulated mini electrode at an applied voltage of 100 mV for duration of 20 minutes and then the experiment was repeated for the collinear double mini electrode and square quadruple mini electrode configurations. These procedures were then also repeated for all the configurations of the insulated mini electrodes. Finally, the surface morphologies of the copper films obtained at the end of the electrodeposition were analyzed using scanning electron microscopy (SEM).

III. RESULTS AND DISCUSSION

A. Transient Current

The transient currents measured for the copper electrodepositions using various designs of mini electrode at 100 mV for duration of 20 minutes are shown in the Fig. 2. The currents measured for all the designs of the uninsulated mini electrodes are higher than the currents measured for all the corresponding sets of insulated mini electrodes. This is because the spread of the electric field from the side of the uninsulated mini electrode disperses copper ions laterally away from the mini electrode and causes the copper ions to be deposited at the regions surrounding the mini electrode. This condition promotes a larger effective growth area and encloses a greater amount of growth centers readily available for deposition, eventually leading to a higher current for the uninsulated mini electrode compare to that of insulated mini electrode. When the number of uninsulated mini electrode is increased from single to collinear double, and then to quadruple configurations, the measured currents were also found to increase with similar trend as that of the single uninsulated mini electrode.

It is noticed that the maximum times (t_{max}) taken to reach the current maxima (I_{max}) for all the uninsulated mini electrodes are much longer than that of the insulated mini electrodes as tabulated in the Table I. This further affirms that the spread of electric field from the side of the uninsulated mini electrode promotes deposition occurs at a larger area surrounding the mini electrode. In addition, the overall charge transfer rate also increases with the larger effective growth area and results in higher current level.

It was observed that the levels of transient currents for the uninsulated mini electrodes are much higher than that of the insulated mini electrodes. These currents were increasing rapidly at the early stage of the electrodeposition processes (less than 3 seconds) and then gradually slowing down before reaching the peak current. After that, the current levels were nearly constant especially for electrodepositions using the single uninsulated and square quadruple uninsulated mini electrodes.

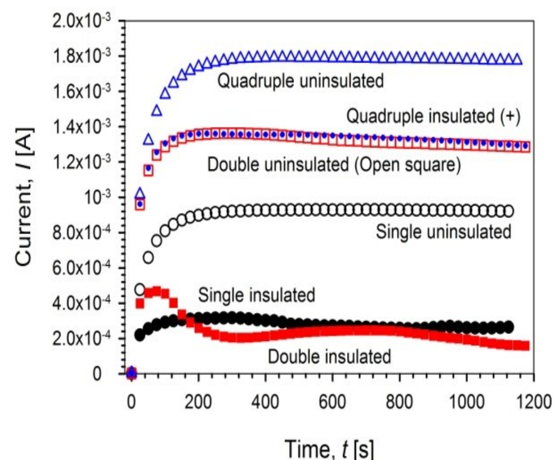

Fig. 2. Transient currents measured for the copper electrodeposition using various designs of mini electrode at 100 mV for duration of 20 minutes. Open and solid symbols represent the electrodeposition carried out with uninsulated and insulated mini electrode, respectively.

Interestingly, the currents measured for single insulated, collinear double insulated, collinear double uninsulated and square quadruple insulated mini electrodes demonstrated multiple current maxima with values lower than the value of the first current maxima despite the fact that they were slowly decreasing with time.

In order to gain better understanding of the dynamic involved in the growth process, the transient current is normalized with its current maxima and re-drawn on a dimensionless plot of square normalized transient current as a function of normalized time [$(I/I_{max})^2$ vs t/t_{max}] as shown in the Fig. 3. The theoretical values of the instantaneous growth and progressive growth based on the diffusion-controlled growth model [18] are also included in the Fig. 3 for comparison. The expressions for the instantaneous growth and progressive growth are written as [18],

For instantaneous growth,

$$\left(\frac{I}{I_{\max}}\right)^2 = \frac{1.9542}{t/t_{\max}}\left[1 - e^{-1.2564(t/t_{\max})}\right]^2 \quad (1)$$

For progressive growth,

$$\left(\frac{I}{I_{\max}}\right)^2 = \frac{1.2254}{t/t_{\max}}\left[1 - e^{-2.3367(t/t_{\max})^2}\right]^2 \quad (2)$$

It was clearly seen that all the electrodepositions conducted using various designs of mini electrodes started with the instantaneous growth mechanism and then lasted for a short period of time before reaching

Table I. Current Maxima and Corresponding Time Maxima for Different Types of Electrodes.

Type of Electrode	t_{max} [s]	I_{max} [A]
Single uninsulated mini electrode	570	9.291×10^{-4}
Single insulated mini electrode	301	4.051×10^{-4}
Collinear double uninsulated minielectrode	292	1.364×10^{-3}
Collinear double insulated mini electrode	74	4.681×10^{-4}
Square quadruple uninsulated mini electrode	422	1.792×10^{-3}
Square quadruple insulated mini electrode	231	1.361×10^{-3}

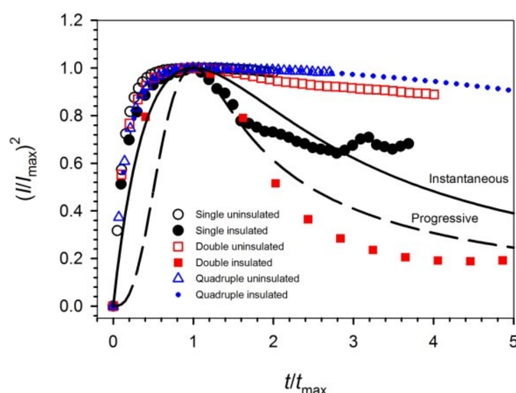

Fig. 3. Dimensionless plot of square normalized transient current as a function of normalized time [$(I/Imax)^2$ vs t/tmax] for copper electrodepositions at 100 mV for duration of 20 minutes. Open and solid symbols represented the electrodepositions carried out with uninsulated and insulated mini electrodes, respectively. The solid line and dashed line represented the theoretical calculation of instantaneous and progressive growths.

the maximum current. In addition, electrodepositions conducted using the insulated mini electrode have lower current levels and then dropped tremendously after reaching the current maxima as compared to that of the uninsulated mini electrode. This trend was quite obvious for the cases of the single and collinear double insulated mini electrodes. For the insulated mini electrode, electric field was constrained to a small area beneath the exposed mini electrode tip. This small region shrank the effective nucleation area and hence reduced the ion exchange activities which yielded lower currents as observed for all the insulated mini electrodes. The localized field beneath the exposed mini electrode tip also helped to promote the overlapping of nuclei at a much shorter time than that of the uninsulated mini electrode and further decreased the current level. This phenomenon is called the progressive growth, where the diffusion zones of the growth centers overlapped and caused the current approached the limiting diffusion current after reaching the current maximum.

Another interesting feature demonstrated by the electrodepositions performed using the single and collinear double insulated mini electrodes are the occurrence of multiple current maxima after the first current maxima. This observation was mainly due to the instantaneous growth superseded the progressive growth. After some times, the progressive growth would then override the instantaneous growth. This pattern occurred repetitively over time and served as the basis for the occurrence of the multiple current maxima after the first current maxima.

As compare to that of the single and collinear double mini electrodes, the normalized transient currents for both the uninsulated and insulated square quadruple mini electrodes did not show significant difference between them. It could be seen that the instantaneous growth mechanism dominated at the beginning of the electrodeposition. The boundary of each growth center was slowly extending with time and increasing the chances of overlapping between growth centers. Thus, competition between progressive growth and instantaneous growth was gradually becoming more frequent and causing the drop in current. This was evidenced through the reoccurrence of current maxima after the first current maxima as shown in the normalized current of the insulated square quadruple mini electrode. Since the normalized currents of the two configurations of the square quadruple mini electrode did not differ significantly, thus the effect of field localization diminished when the number of insulated mini electrode was increased. This imitated the deposition using a very large number of mini electrodes that were closely packed together making the mini electrodes to resemble a planar electrode that exerted parallel electric field on the substrate during the deposition.

B. Surface Morphology

Surface morphologies of the copper films that were located at the area beneath the tip of a single uninsulated mini electrode and a single insulated mini electrode were shown the Fig. 4(a) and Fig. 5(a), respectively. It could be seen that surface area beneath the tip that was exposed to the large localized electric field emitting from the tip was heavily deposited with copper ions starting along the edge of the ridges and rapidly expanded to the side of the ridges. Eventually, valleys between the ridges were filled up with copper atoms and the ridges seemed to merge together and covered the whole surface areas beneath the tip. The high deposition rate due to the large localized electric field that was emitting from the tip had induced the progressive growth at the

Table II. Root-Mean-Square Surface Roughness, *R*q of Copper Films Obtained for Depositions Using Different Mini Electrodes.

Type of Electrode	Beneath the Tip [nm]	Away From the Tip [nm]
Single uninsulated mini electrode	178.5	207.6
Single insulated mini electrode	177.2	200.6
Collinear double uninsulated minielectrode	182.7	199.4
Collinear double insulated mini electrode	188.6	156.6
Square quadruple uninsulated mini electrode	150.1	148.9
Square quadruple insulated mini electrode	166.6	104.1

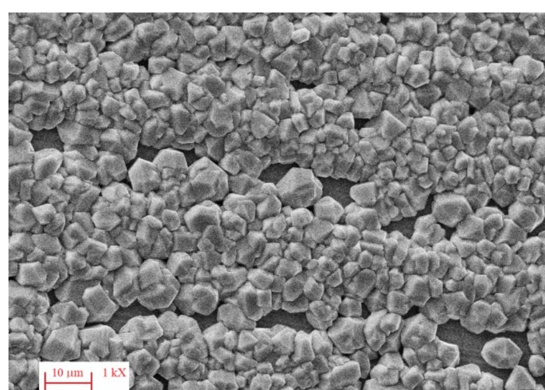

(a)

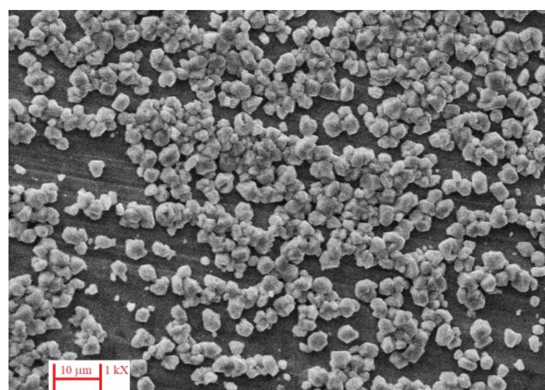

(b)

Fig. 4. Surface morphologies that were located (a) beneath and (b) away from the tip of a single uninsulated mini electrode.

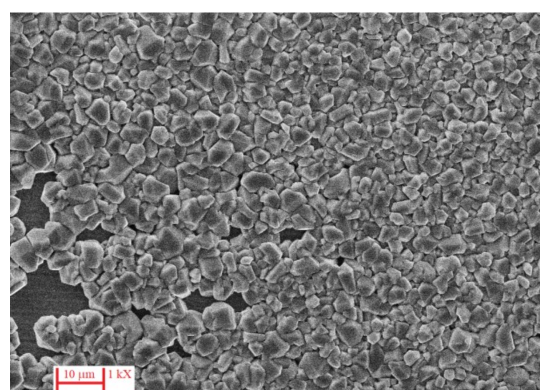

(a)

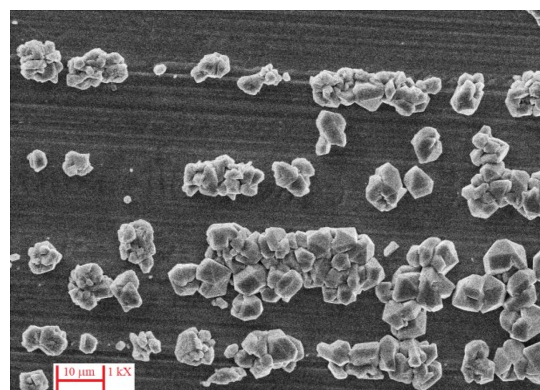

(b)

Fig. 5. Surface morphologies that were located (a) beneath and (b) away from the tip of a single insulated mini electrode.

beginning of the deposition process. When progressive growth occurred, nuclei had a tendency to deposit on each other, instead of growing at the kink sites on the surface of the copper film. At the same time, the overlapping of nuclei also hindered the subsequent growth process which then caused the drop of the transient current especially for the deposition that was carried out using the single insulated mini electrode as shown in the Fig. 3.

Surface morphologies of the copper films that were located away from the copper tip of a single uninsulated mini electrode and a single insulated mini electrode were shown in the Fig. 4(b) and Fig. 5(b), respectively. For single uninsulated mini electrode, the spread of electric field from the side of the mini electrode caused copper ions to flow laterally in the electrolyte some distances away from the mini electrode. When copper ions arrived near the surface of the copper film, they deposited along the edge of the ridges. After some times, the growth area was gradually expanding to the valleys between the ridges and copper ions were then covering up partial surface areas of the copper film as depicted in the Fig. 4(b). The continuation of deposition of copper ions at the areas away from the mini electrode explained the constant transient current behavior of the single uninsulated mini electrode as shown in the Fig. 2.

For the single insulated mini electrode, there was still a small amount of copper ions diffused laterally on the surface of the copper film and adsorbed at the areas away from the tip. The dispersion of these copper ions was due to the diverging electric fields

from the tip of the insulated mini electrode. However, the lateral distance travelled by the copper ions of the single insulated mini electrode is shorter than that of the single uninsulated mini electrode. Hence, there was only a small fraction of the surface area of the copper film was deposited (as shown in the Fig. 5(b)) and the transient current could not be sustained as compared to that of the single uninsulated mini electrode. It could be seen that the surface roughness measured at the area away from the mini electrode is larger than the surface roughness measured at the area beneath the tip (see the Table II). This could be explained as the electric field was sparsely distributed at the area away from the mini electrode and caused formation of different sizes of cluster of atoms along the edge of the ridges on the copper film as shown in the Fig. 4(b) and Fig. 5(b).

Figure 6(a) and Fig. 7(a) showed the surface morphologies located beneath the tips of the collinear double uninsulated mini electrode and the collinear double insulated mini electrode. Both surfaces were heavily deposited and fully coated with copper atoms. In comparison, the localized electric field emitted from the tips of the collinear double mini electrode covered a larger area than that of the single mini electrode as the number of mini electrodes increased. Thus, it was expected that the onset of progressive growth during the deposition using collinear double mini electrode was faster than that of the single mini electrode as shown in the Fig. 1 and Table I. Higher deposition rate produced rougher surface for the collinear double mini electrode as compared to that of the single mini electrode as indicated by the RMS values in the Table II.

Figure 6(b) and Fig. 7(b) showed the surface morphologies located away from the copper tips of the collinear double uninsulated mini electrode and the collinear double insulated mini electrode. Although the electric fields established in the interspacing between the collinear double uninsulated mini electrodes were compensated, but the spread of electric field still occurred at the outermost field region of the uninsulated mini electrodes which was also larger than that of the single uninsulated mini electrode. This encouraged a large amount of copper ions were dispersed far away from the side of the collinear double uninsulated mini electrode and deposited on the copper film via the progressive growth dynamics. Hence, this area was heavily deposited with copper ions compared to that of the single uninsulated mini electrode as shown in Fig. 6(b). Due to the progressive growth, the transient current was decreasing over time though multiple instantaneous growths were occasionally observed when copper ions were trying to fill up the empty regions on the cooper film. These empty regions caused uneven surface and yielded a rougher surface at the area away from the tips than that of the area

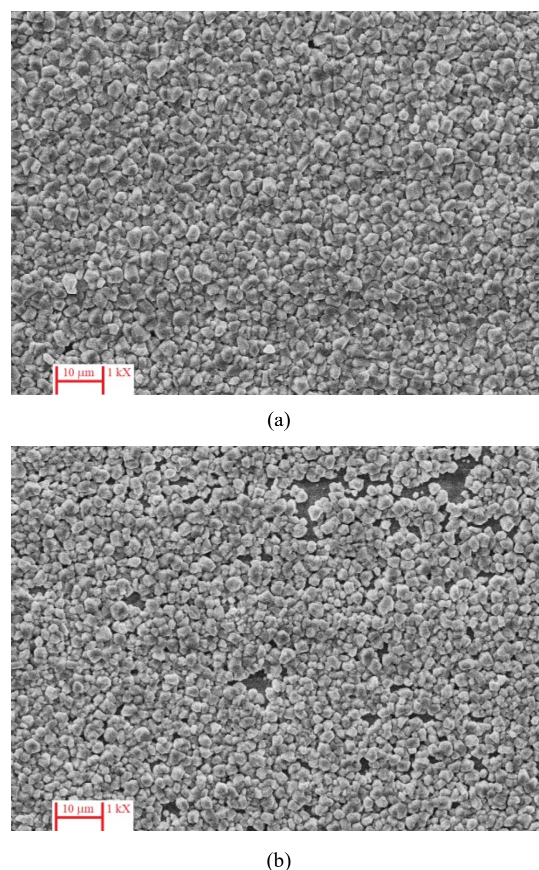

Fig. 6. Surface morphologies located (a) beneath and (b) away from the tip of the collinear double uninsulated mini electrode.

near the tips of the collinear double uninsulated mini electrode as tabulated in the Table II.

For the collinear double insulated mini electrode, most of the copper ions were deposited beneath the tips due to the high localized electric field. This led to the occurrence of overlapping of nuclei during the growth and hindered the subsequent deposition of copper ions. This caused the transient current was decreasing with time. It was observed that the surface roughness measured at the area away from the tips is significantly smaller than the surface roughness measured at the area near the tips of the collinear double insulated mini electrode at tabulated in the Table II. This was because there were only very small amount of copper ions diffused away from the tips and sporadically coated on the surface of the copper film as shown in Fig. 7(b). Thus, the measured surface roughness represented the surface roughness of the substrate of the copper film.

Figure 8 and Fig. 9 showed the surface morphologies of the copper films located at the area beneath the copper tips of the square quadruple uninsulated mini electrode and square quadruple insulated mini electrode. Surface morphologies of the copper film obtained from the area far away from the copper tips were similar to surface morphologies

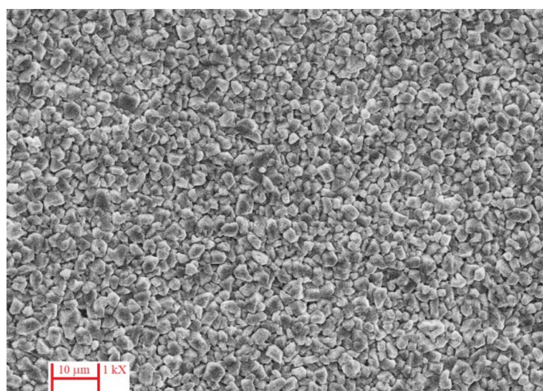

(a)

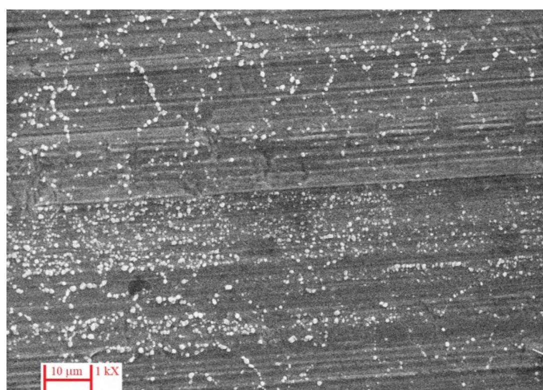

(b)

Fig. 7. Surface morphologies located (a) beneath and (b) away from the tips of the collinear double insulated mini electrode.

obtained at the area beneath the tips, thus they were not shown in the manuscript. Electric fields of the uninsulated mini electrode at the interspacing between the mini electrodes were diminished when the number of mini electrode was increased but electric field still extended from the outermost field region. Copper ions that arrived near the outermost field region of the uninsulated mini electrode would be dispersed to the side of the uninsulated mini electrode. Thus, a larger area was involved during the deposition process and allowed more ion exchange activities occurred when copper ions formed on the surface of the copper films. This helped to sustain the transient current and yielded a higher current level as compared to that of the deposition carried out using insulated mini electrode as shown in the Fig. 2. In contrast, the electric field of the insulated mini electrode was highly localized near the tips thus copper ions had a tendency to deposit at the region near to the tips and promoted the overlapping effect which hindered the deposition process. This explained why the transient current measured for the deposition using insulated mini electrode was decreasing with time. The surface roughness value obtained for the deposition carried out using the square quadruple insulated mini electrode was slightly larger than that of the deposition carried out using the square quadruple uninsulated mini

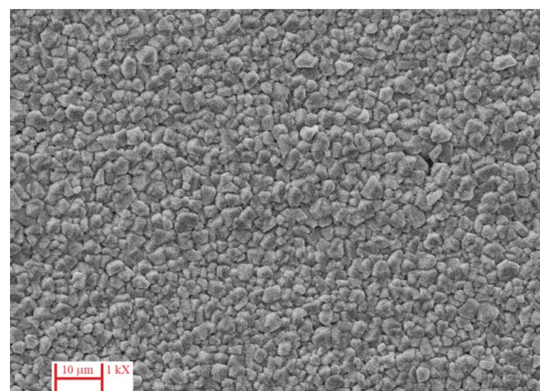

Fig. 8. Surface areas located beneath and away from the tip of the square quadruple uninsulated mini electrode presented similar surface morphologies.

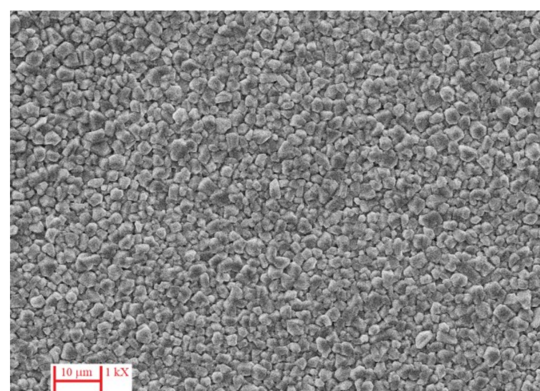

Fig. 9. Surface areas located beneath and away from the tips of the square quadruple insulated mini electrode presented similar surface morphologies.

electrode. This was simply due to the occurrence of the overlapping effect during the deposition process using the insulated mini electrode. In addition, the localized electric fields at the tips of the square quadruple uninsulated mini electrode and the square quadruple insulated mini electrode became more uniform as the number of mini electrode was increased. This led to a more uniform deposition of the copper ions on the surface of the copper film and yielded a relative smoother surface with smaller surface roughness values (see Table II) as compared to that of the deposition carried using either single or collinear double mini electrode.

IV. CONCLUSION

Insulated mini electrode localized and concentrated electric field within the area beneath the tip of the mini electrode. The localization of electric field yielded high deposition rate of copper ions within this area. This encouraged the progressive growth set in faster and easier for the deposition performed using the insulated mini electrode and hindered the subsequent nuclei growth process. Insulated mini electrode restricted the electric field to the tip, thus the dispersion of copper ions to the side

of the insulated mini electrode is greatly reduced compared to that of the uninsulated mini electrode. Because of that, the measured transient current of the deposition using insulated mini electrode decreased with time. In contrast, the measured transient current of the uninsulated mini electrode was sustaining with time when copper ions were dispersed away and deposited on the areas far from the mini electrode before the progressive growth set in again. Since copper ions sporadically deposited on the area far from the mini electrode, thus deposition performed using the single or double mini electrode tended to produce isolated structures with rougher surface. However, it was observed that the deposition performed using multiple or a large number of closely spaced mini electrodes tended to produce a copper film with more uniform and smoother surface due to the electric field pattern produced by a large number of closely spaced mini electrodes resembled the parallel and uniform electric field pattern of a flat copper film. Owing to the flexibility of anode design and configuration, localized electrodeposition using miniature electrode has great potential to be applied in realizing direct 3D printing, MEMS, NEMS, or complex structure of metal contacts of semiconductor or optoelectronic devices.

ACKNOWLEDGEMENT

The authors are extremely grateful to the Ministry of Higher Education (MOHE) of Malaysia for financial support through the Fundamental Research Grant Scheme (FRGS/2/2010/SG/MMU/02/5) and Dr. Lim Weng Lee for helping out in the SEM imaging.

REFERENCES

[1] R. J. Nichols, D. Schroer and H. Meyer, "An In-Situ Scanning Probe Microscopy Study of Copper Electrodeposition on Conductive Polypyrrole," *Electrochim. Act.*, vol. 40, pp. 1479-1485, 1995.

[2] P .C. Andricacos, "Copper On-Chip Interconnections A Breakthrough in Electrodeposition to Make Better Chips," *Electrochem. Soc. Interface*, vol. 8, pp. 32-37, 1999.

[3] W. Schwarzacher, "Electrodeposition: A Technology for The Future," *Electrochem. Soc. Interface*, vol. 15, pp. 32-35, 2006.

[4] W. C. Gau, T. C. Chang, Y. S. Lin, J. C. Hu, L. J. Chen, C. Y. Chang and C. L. Cheng, "Copper Electroplating For Future Ultralarge Scale Integration Interconnection," *J. Vac. Sci. Technol. A*, vol. 18, pp. 656-660, 2000.

[5] G. C. Schwartz and K. V. Srikrishnan, "Handbook of Semiconductor Interconnection Technology," Second ed., *CRC Press*, Boca Raton, U.S.A, 2006.

[6] T. Gupta, "Copper Interconnect Technology," *Springer*, New York, U.S.A., 2009.

[7] J. D. Madden and I. W. Hunter, "Three-dimensional Microfabrication by Localized Electrochemical Deposition," *J. Microelectromech. Syst.*, vol. 5, pp. 24-32, 1996.

[8] I. Schönenberger and S. Roy, "Microscale Pattern Transfer Without Photolithography of Substrates," *Electrochim. Acta*, vol. 51, pp. 809-819, 2005.

[9] Q. B. Wu, T. A. Green and S. Roy, "Electrodeposition of Microstructures Using a Patterned Anode," *Electrochem. Commun.*, vol. 13, pp. 1229-1232, 2011.

[10] D. M. Kolb, R. Ullmann and J. C. Ziegler, "Electrochemical Nanostructuring," *Electrochim. Acta*, vol. 43, pp. 2751-2760, 1998.

[11] P. Möller, M. Fredenberg, M. Dainese, C. Aronsson, P. Leisner and M. Östling, "Metal Printing of Copper Interconnects Down to 500 nm Using ECPR: Electrochemical Pattern Replication," *Microelectron. Eng.*, vol. 83, pp. 1410-1413, 2006.

[12] H. A. Murdoch, D. Yin, E. H. Rivera and A. K. Giri, "Effect of Applied Magnetic Field on Microstructure of Electrodeposited Copper," *Electrochem. Commun.*, vol. 97, pp. 11-15, 2018.

[13] D. Fernández, M. Martine, A. Meagher, M. E. Möbius and J. M. D. Coey, "Stabilizing Effect of A Magnetic Field on A Gas Bubble Produced at A Microelectrode," *Electrochem. Commun.*, vol. 18, pp. 28-32, 2012.

[14] L. M.A. Monzon and J. M. D. Coey, "Magnetic Fields in Electrochemistry: The Lorentz Force. A Mini-Review," *Electrochem. Commun.*, vol. 42, pp. 38-41, 2014.

[15] L. M.A. Monzon and J. M. D. Coey, "Magnetic Fields in Electrochemistry: The Kelvin Force. A Mini-Review," *Electrochem. Commun.*, vol. 42, pp. 42-45, 2014.

[16] H. Fan, Y. Zhao, S. Wang and H. Guo, "Effect of Jet Electrodeposition Conditions on Microstructure and Mechanical Properties of Cu-Al^2O_3 Composite Coatings," *Int. J. Adv. Manuf. Technol*., vol. 105, pp. 4509-4516, 2019.

[17] H. Fan, Y. Zhao, J. Jiang, S. Wang, W. Shan and R. Ma, "Pulse Jet Electrodeposition of Nanocrystalline Copper and its Application as an Electrical Discharge Machining Electrode," *Int. J. Electrochem. Sci.*, vol. 15, pp. 2648-2658, 2020.

[18] B. Scharifker and G. Hills, "Theoretical and Experimental Studies of Multiple Nucleation," *Electrochim. Acta*, vol. 28, pp. 879-889, 1983.